

Observation of spinor dynamics in optically trapped ^{87}Rb Bose-Einstein Condensates

M.-S. Chang, C. D. Hamley, M. D. Barrett,* J. A. Sauer, K. M. Fortier, W. Zhang, L. You, and M. S. Chapman
*School of Physics, Georgia Institute of Technology,
Atlanta, Georgia 30332-0430*
(Dated: September 15, 2018)

We measure spin mixing of $F=1$ and $F=2$ spinor condensates of ^{87}Rb atoms confined in an optical trap. We determine the spin mixing time to be typically less than 600 ms and observe spin population oscillations. The equilibrium spin configuration in the $F=1$ manifold is measured for different magnetic fields and found to show ferromagnetic behavior for low field gradients. An $F=2$ condensate is created by microwave excitation from $F=1$ manifold, and this spin-2 condensate is observed to decay exponentially with time constant 250 ms. Despite the short lifetime in the $F=2$ manifold, spin mixing of the condensate is observed within 50 ms.

PACS numbers: 03.75.Mn, 32.80.Pj, 03.67.-a

One of the hallmarks of Bose-Einstein condensation (BEC) in dilute atomic gases is the relatively weak and well-characterized inter-atomic interactions that allow quantitative comparison with theory. The vast majority of experimental work has involved single component systems, using magnetic traps confining just one Zeeman sub-level in the ground state hyperfine manifold. An important frontier in BEC research is the extension to multi-component systems, which provides a unique opportunity for exploring coupled, interacting quantum fluids. In particular, atomic BECs with internal spin degrees of freedom offer a new form of coherent matter with complex internal quantum structures. The first two-component condensate was produced utilizing two hyperfine states in ^{87}Rb , and remarkable phenomena such as phase separation were observed [1, 2]. Sodium $F=1$ spinor BECs have been created by transferring spin polarized condensates into a far-off resonant optical trap to liberate the internal spin degrees of freedom. This allowed investigations of the ground state properties of Na spinor condensates, and observations of domain structures, metastability, and quantum spin tunneling [3, 4, 5].

In this letter, we explore the spin dynamics and ground state properties of ^{87}Rb spinor condensates in an all-optical trap, by starting with well-characterized initial conditions in a known magnetic field. We focus on the $F=1$ case and confirm the predicted ferromagnetic behavior. We observe population oscillation between different spin states during the spin mixing and observe reduced magnetization fluctuations, pointing the way to future exploration of the underlying spin squeezing and spin entanglement predicted for the system [6]. We also create $F=2$ spinors using a microwave excitation, measure a decay of the condensate with a time constant of 250 ms. Despite the short lifetime, spin mixing of the spin-2 condensates is observed within 50 ms. Similar results are concurrently reported in Ref [7]; in that work, the emphasis is on the $F=2$ mixing, while here, we focus mainly on the $F=1$ manifold.

A spinor BEC can be described by a multi-component

order parameter which is invariant under gauge transformation and rotation in spin space [8, 9, 10]. For a spin-1 BEC, the condensate is either ferromagnetic or anti-ferromagnetic [8], and the corresponding ground state structure and dynamical properties of these two cases are very distinct. The Na $F=1$ spinor was found to be anti-ferromagnetic, while the $F=1$ ^{87}Rb is predicted to be ferromagnetic [11, 12]. Even richer dynamics are predicted for spin-2 condensates [13], although they remain largely unexplored experimentally [7, 14].

Single component BECs are typically well-described by a scalar order parameter $\psi(\mathbf{r}, t)$ (the BEC “wavefunction”) whose dynamics is governed by the nonlinear Gross-Pitaevskii equation [15], $i\hbar\frac{\partial\psi}{\partial t} = -\frac{\hbar^2}{2m}\nabla^2\psi + V_t\psi + c_0|\psi|^2\psi$, where V_t is the trap potential, c_0 the two-body mean field interaction coefficient, and $|\psi|^2 = n$ is the density. For spinor condensates, the Bogoliubov formalism can be extended to a vector order parameter ψ_χ , where χ is the spin vector with $2F+1$ components for spin- F condensates [8, 9]. For $F=1$, the two-body interaction energy including spin is $U(r) = \delta(r)(c_0 + c_2\mathbf{F}_1 \cdot \mathbf{F}_2)$, where r is the distance between two atoms and c_2 is the spin dependent mean-field interaction coefficient. For $F=2$, $U(r) = \delta(r)(\alpha + \beta\mathbf{F}_1 \cdot \mathbf{F}_2 + 5\gamma P_0)$, where α is a spin-independent coefficient, β and γ are spin-dependent coefficients, and P_0 is the projection operator [8, 9].

The spin-1 ground states have been calculated by several groups for both zero magnetic field [8, 10] and finite field cases [16]. Although the spin dependent terms, e.g. $|c_2|$, are typically one to two orders of magnitude less than the spin independent mean field interaction $|c_0|$, they can have a dramatic effect on the ground state structure and dynamical properties of the condensates. Ho showed that if c_2 is negative (positive), the spinor displays ferromagnetic (anti-ferromagnetic) behavior [8]. For the case of $F=1$ ^{87}Rb , c_2 is calculated to be $-3.58(57)\times 10^{-20}\text{Hz} \cdot \text{m}^3$ [12]. Hence the ground state of ^{87}Rb should be ferromagnetic [11] with a global minimal energy state at zero field of $|F=1, m_F=1\rangle$ [8].

For finite fields, the ferromagnetism will manifest it-

self in different ways depending on the scale of the ferromagnetic energy compared with the Zeeman energy. For a typical density of $n = 4 \times 10^{14} \text{ cm}^{-3}$ in our optical traps, the ferromagnetic energy $2|c_2|n$ is only 28 Hz [3], and hence, observation of the low field ground state, $|F = 1, m_F = 1\rangle$, requires that the first order (linear) Zeeman shift $E_Z = m_F B \times (700 \text{ Hz/mG})$ be smaller than $2|c_2|n$, and hence requires zeroing the magnetic field B to less than $40 \mu\text{G}$, typically requiring a magnetically shielded environment.

Even at much larger fields (up to $\sim 500 \text{ mG}$ in our case), however, the ferromagnetic interactions can still play a dominant role in determining the spin ground state due to constraints imposed by angular momentum conservation. If we start with a non-equilibrium spin mixture, the system will relax to the minimal energy state via spin exchange collisions, and for the $F=1$ manifold, the only processes that conserve angular momentum are

$$2|m_0\rangle \rightleftharpoons |m_1\rangle + |m_{-1}\rangle. \quad (1)$$

Hence, the normalized magnetization of the system $M = n_1 - n_{-1}$ is a conserved quantity, where n_i is the fraction of condensate atoms in the i th Zeeman state m_i , and for a given M , the system is uniquely determined by n_0 . In this field regime, the effect of the anti-ferromagnetism (ferromagnetism) is to lower (raise) the energy of the m_0 spinor component relative to the average energy of the $m_{\pm 1}$ components [3], which drives the reaction in Eq. 1 to the left (right). Hence, the extent to which this reaction is driven provides an unambiguous distinction between the ferro- and anti-ferromagnetic cases. At higher fields, these effects compete with the second order (quadratic) Zeeman shift, $(E_{+1} + E_{-1} - 2E_0)/2 \simeq B^2 \times (350 \text{ Hz/G}^2)$ [3], which tends to drive the reaction to the left (to the m_0 state) for fields $B \gtrsim 500 \text{ mG}$. Although evidence of the ferromagnetism of ^{87}Rb was already provided by the observed spin mixtures in our previous work (which were measured at $\sim 100 \text{ mG}$) [17, 18], and currently reported by Ref. [7] (which are measured at $\sim 340 \text{ mG}$), here we present systematic studies of the spin mixing, starting with non-equilibrium initial conditions and following its time evolution for different magnetic fields.

Our experiments employ an all-optical BEC technique previously described in [17]. The atoms are loaded directly from a magneto-optical trap into an optical dipole force trap formed by a CO_2 laser. Lowering the laser power forces evaporative cooling in the optical trap, leading to rapid condensation. In this work, we employ a large period ($5.3 \mu\text{m}$) 1-D lattice made by a CO_2 laser standing wave [18] which provides a strongly anisotropic pancake shape trap, allowing clear distinction between thermal clouds and condensates. The lattice is loaded by transferring atoms from an orthogonal travelling wave trap. We create condensates in only one lattice site by

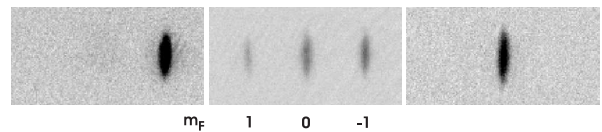


FIG. 1: By applying different magnetic field gradients at different stages of evaporation, we can create pure condensates of a particular spin or mixtures, which consists of 30,000 to 15,000 atoms as seen above. Each absorptive image is taken after 6 ms of free expansion, and a weak Stern-Gerlach field is applied during the first 2 ms of expansion to separate three spin components spatially. The field of view of each image is $460 \times 230 \mu\text{m}$.

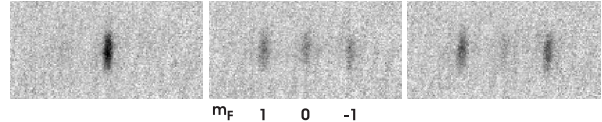


FIG. 2: Spin mixing of spinor condensate in the optical trap. The mixing process starts with a pure $m_F = 0$ condensate in the optical trap. Three separate measurements of the spin state are shown after 2 s of spin mixing.

adjusting the trap power during transfer. The condensates contain 30,000 atoms in a single lattice site with measured trap frequencies $2\pi(120, 120, 2550) \text{ rad/s}$, and no observable thermal component. The density in the optical trap is estimated to be $4.3 \times 10^{14} \text{ cm}^{-3}$, and the Thomas-Fermi condensate radii are $(7.6, 7.6, 0.36) \mu\text{m}$. The $1/e$ lifetime of the condensates in our optical trap is about 3 s.

To control the initial spin population, we apply different magnetic field gradients during the evaporation process [18]. To create a pure $F = 1, m_F = 0$ condensate, we apply a field gradient of 28 G/cm during the final 1 s of evaporation. To create an equally mixed $m_F = -1, 0, 1$ condensate, a smaller gradient (14 G/cm) is applied. We can also create a pure $m_F = -1$ by applying a 28 G/cm gradient at an earlier time before the transfer to the lattice. Typical spinor condensates with different spin configurations are illustrated in Figure 1.

To study the spin mixing dynamics, we begin with pure $m_F = 0$ condensates as the initial condition. After condensation, the field gradient is turned off, and a variable magnetic bias field is adiabatically ramped up in 10 ms. This field can be directed either along the tight (axial) or weak (radial) axes of the confinement potential. The condensate is then allowed to evolve for a variable amount of time, and then the spin populations are measured using absorptive imaging following 6 ms of free expansion. To spatially separate the spin components, a weak Stern-Gerlach field is applied during the first 2 ms of expansion. Typical results for 2 s of spin mixing are shown in Figure 2. We note from these three images taken under identical conditions that there is significant variation on the degree

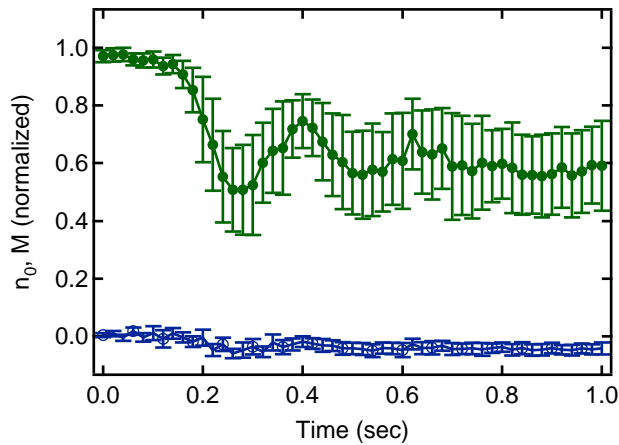


FIG. 3: Plot of the fraction in the $m_F=0$ state n_0 and magnetization M (open circle) vs. time. In this measurement, M is determined to be $0.5\pm 0.8\%$ initially and $-3.5\pm 2\%$ after mixing. Note that there is a 8.5-fold reduction on the fluctuation of M compare to that of the total population (which is measured to be 17%). Clear population oscillations of n_0 are seen, and the fluctuation in n_0 is 6.6 fold of that of M . This data was taken at a bias field of 100 mG

of mixing from run to run of the experiment. However, in each case, the magnetization appears to be conserved. Generally, the components of the spin mixtures are identical in shape to the original cloud to within our imaging resolution. Occasionally one or more of the components will appear to have either a thermal component or a distorted shape.

We have measured the spin mixing for different evolution times following preparation of the $m_F = 0$ condensates. The time to reach equilibrium of the spin mixing is typically less than 600 ms, and this time decreases slightly with increasing magnetic field. Fig. 3 shows the average time evolution of n_0 and M for 50 repeated measurements. First, we note that the magnetization, M , is conserved throughout the mixing to within a few percent. Although the data does suggest a drift of M below zero by a small amount $-3.5\pm 2\%$ (the uncertainty here and error bars in the data are purely statistical), the deviation, if any, is comparable to our uncertainties in measuring populations ($\sim 3\%$), limited by the absorptive imaging technique. Secondly, there is an almost 10-fold reduction in the statistical noise of the magnetization relative to that of the total population, which varies 17% from shot to shot. This suggests that the fluctuations of n_1 and n_{-1} , which are coupled from the mixing processes in Eq. (1), are quantum correlated. These correlations underly theoretical predictions for spin squeezing and entanglement in the system [6]. Thirdly, the relaxation of n_0 to the steady state value is not monotonic but instead shows a damped oscillation at 4 Hz. Such oscillations are a natural outcome of coherent spinor mixing as shown theoretically in [19].

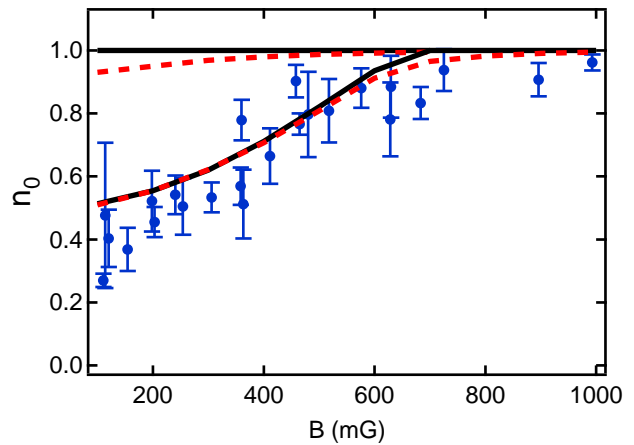


FIG. 4: Plot of n_0 vs. magnetic field after 3 s of spin mixing. The upper curves are the theoretical predictions for the anti-ferromagnetic case, while the lower curves are for the ferromagnetic case. The dashed lines are the predictions with a field of gradient 20 mG/cm applied, which is the measured upper bound in our trap.

We attempted to directly measure the phase relationship between the spinor components [20] by performing an interference experiment between two spinor condensates created in adjacent lattice sites. In the absence of dephasing mechanisms, we would expect to see clear interference fringes in time-of-flight measurements both before and after spin mixing. In the measurement, clear interference fringes were visible initially, while fringes were typically not observed after mixing. It is quite possible however that the observed dephasing of the interference pattern was caused by small field variations between two sites due to a stray magnetic field gradient (< 20 mG/cm) [21].

To make comparison with theoretical predictions [16], we measure the degree of mixing for different applied magnetic fields. Fig. 4 shows the results of spin mixing for 3 s, in which n_0 is plotted vs. the applied field. Also shown in this figure are theoretical curves for both the antiferro- and ferromagnetic cases in a magnetic field with and without a small (20 mG/cm) field gradient [16]. As evidenced by the data, the spin mixing agrees with the ferromagnetic predictions and is inconsistent with the anti-ferromagnetic prediction. When the field is larger than 700 mG, the quadratic Zeeman effect completely dominates the spin interaction, and the condensates remain in the $m_F = 0$ state. Note that magnetic fields are applied either along tight trap or weak trap axes with different polarities; however, no significant difference in the measurements is observed.

We also measured spin mixing for fields less than 100 mG but found that our results were affected by the stray ~ 10 mG AC magnetic fields present in the chamber. These fields are capable of driving off-resonant rf

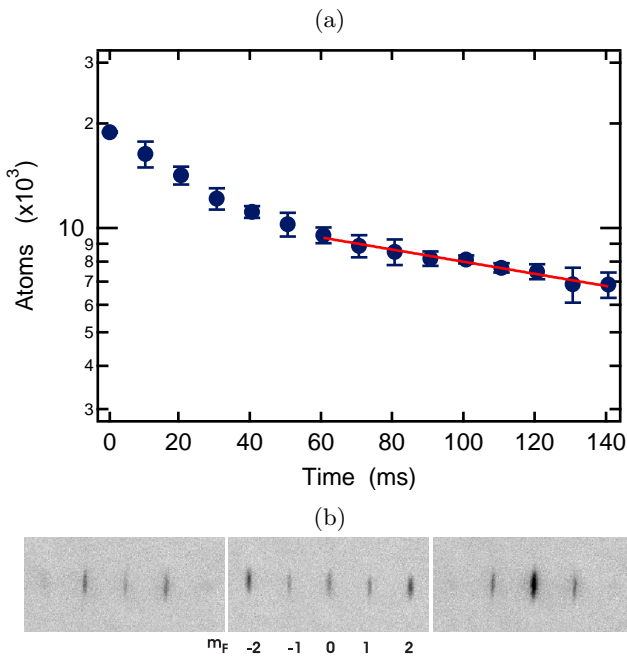


FIG. 5: (a) Lifetime measurement of $F=2$ spinor condensates. Following a rapid decay initial decay, the population decays exponentially with a time constant of 250 ms. (b) Spin mixing of the $F=2$ spinor condensates in the optical trap. These images represent three identical measurements after 50 ms of spin mixing. Note that the magnetization is conserved.

transitions between the Zeeman sub-levels. We observed this directly by creating a $F = 1, m_F = -1$ condensate (for which there is no spin mixing due to conservation of magnetization) and measuring the final spin population. For magnetic fields greater than 100 mG, the magnetization remains conserved, while at lower fields, the $m_F = -1$ atoms are quickly pumped by the AC fields (within 100 ms for fields < 10 mG) to other Zeeman states.

To study $F=2$ spinors, we coherently excite the pure $F = 1, m_F = 0$ condensates to $F = 2, m_F = 0$ using microwave fields tuned to 6.8 GHz. Additionally, by controlling the bias field, the microwave frequency, and the initial Zeeman state in the $F=1$ manifold, we can pump the condensate to any Zeeman sub-level of the excited hyperfine manifold. The $F=2, m=0$ condensate is observed to decay as shown in Fig 5(a). Following an initially rapid decay, it decays exponentially with a time constant of 250 ms. Despite the short lifetime in the excited hyperfine manifold, we still observe spin mixing within 50 ms, and magnetization conservation is also observed during the mixing, as shown in Fig. 5(b).

In summary, we have observed spin mixing of ^{87}Rb spinor condensates in $F=1$ and $F=2$ hyperfine manifolds in an optical trap. The observed equilibrium spinor configurations of the lower manifold confirms that $F=1$ ^{87}Rb is ferromagnetic. The magnetization was conserved

within the measurement errors during the entire spin mixing process. The reduced noise of magnetization suggests quantum correlation of the spin dynamics, which underlies spin squeezing and spin entanglement. Future work will study the coherence of spin mixing, spin squeezing, and entanglement.

We acknowledge valuable discussions with L.-T. Ho, T. A. B. Kennedy, A. Kuzmich, H. Pu, C. Raman, and S. Yi. This work is supported by NASA Grant No. NAG3-2893. and by NSF Grant No. PHY-0303013.

* Current address NIST, Boulder, CO.

- [1] C. J. Myatt, E. A. Burt, R. W. Ghrist, E. A. Cornell, and C. E. Wieman, *Phys. Rev. Lett.* **78**, 586 (1997).
- [2] E. A. Cornell, D. S. Hall, M. R. Matthews, and C. E. Wieman, *J. Low Temp. Phys.* **113**, 151 (1998).
- [3] J. Stenger *et al.*, *Nature* **396**, 345 (1998).
- [4] H.-J. Miesner *et al.*, *Phys. Rev. Lett.* **82**, 2228 (1999).
- [5] D. M. Stamper-Kurn *et al.*, *Phys. Rev. Lett.* **83**, 661 (1999).
- [6] L. You, *Phys. Rev. Lett.* **90**, 030402 (2003).
- [7] H. Schmaljohann *et al.*, *cond-mat/0308281*, (2003).
- [8] T.-L. Ho, *Phys. Rev. Lett.* **81**, 742 (1998).
- [9] T. Ohmi and K. Machida, *J. Phys. Soc. Jpn.* **67**, 1822 (1998).
- [10] C. K. Law, H. Pu, and N. P. Bigelow, *Phys. Rev. Lett.* **81**, 5257 (1999).
- [11] N. N. Klausen, J. L. Bohn, and C. H. Greene, *Phys. Rev. A* **64**, 053602 (2001).
- [12] E. G. M. van Kempen, S. J. J. M. F. Kokkelmans, D. J. Heinzen, and B. J. Verhaar, *Phys. Rev. Lett.* **88**, 093201 (2002).
- [13] C. V. Ciobanu, S.-K. Yip, and T.-L. Ho, *Phys. Rev. A* **61**, 033607 (2000).
- [14] A. Görlitz *et al.*, *Phys. Rev. Lett.* **90**, 090401 (2003).
- [15] C. J. Pethick and H. Smith, *Bose-Einstein Condensation in dilute Gases*, (Cambridge University Press, Cambridge, UK, 2002)
- [16] W. Zhang, S. Yi, and L. You, *New Journal of Physics* **5**, 77.1 (2003).
- [17] M. D. Barrett, J. A. Sauer, and M. S. Chapman, *Phys. Rev. Lett.* **87**, 010404 (2001).
- [18] M. D. Barrett *et al.*, in *Proceedings of the XVII International Conference on Atomic Physics (ICAP2002)*, edited by H. R. Sadeghpour, E. J. Heller, and D. E. Pritchard (World Scientific, Singapore, 2003), p. 31. (1961)]; M. D. Barrett *et al.* (to be published).
- [19] H. Pu, C. K. Law, S. Raghavan, J. H. Eberly, and N. P. Bigelow, *Phys. Rev. A* **60**, 1463 (1999).
- [20] T. Isoshima, T. Ohmi, and K. Machida, *J. Phys. Soc. Jpn.* **69**, 3864 (2000).
- [21] To determine magnetic fields at trap location, we employ microwave spectroscopy on the field sensitive $F=1 \rightarrow F=2$ hyperfine transitions which is sensitive to within 2 mG. Furthermore, the field gradient is determined to be < 20 mG/cm by measuring fields at different trap locations.